Published in final edited form as:
Int Forum Allergy Rhinol. 2013 January ; 3(1): 48–55. doi:10.1002/alr.21070.

Computed Intranasal Spray Penetration: Comparisons Before and After Nasal Surgery

Dennis O. Frank, Ph.D.[1], **Julia S. Kimbell, Ph.D.**[1], **Daniel Cannon, M.D.**[2], and **John S. Rhee, M.D., M.P.H.**[2]

[1]Department of Otolaryngology/Head and Neck Surgery, University of North Carolina, Chapel Hill, North Carolina

[2]Departments of Otolaryngology and Communication Sciences, Medical College of Wisconsin, Milwaukee, Wisconsin

Abstract

Background—Quantitative methods for comparing intranasal drug delivery efficiencies pre- and postoperatively have not been fully utilized. The objective of this study is to use computational fluid dynamics techniques to evaluate aqueous nasal spray penetration efficiencies before and after surgical correction of intranasal anatomic deformities.

Methods—Ten three-dimensional models of the nasal cavities were created from pre- and postoperative computed tomography scans in five subjects. Spray simulations were conducted using a particle size distribution ranging from 10–110μm, a spray speed of 3m/s, plume angle of 68°, and with steady state, resting inspiratory airflow present. Two different nozzle positions were compared. Statistical analysis was conducted using Student T-test for matched pairs.

Results—On the obstructed side, posterior particle deposition after surgery increased by 118% and was statistically significant (p-value=0.036), while anterior particle deposition decreased by 13% and was also statistically significant (p-value=0.020). The fraction of particles that by-passed the airways either pre- or post-operatively was less than 5%. Posterior particle deposition differences between obstructed and contralateral sides of the airways were 113% and 30% for pre- and post-surgery, respectively. Results showed that nozzle positions can influence spray delivery.

Conclusions—Simulations predicted that surgical correction of nasal anatomic deformities can improve spray penetration to areas where medications can have greater effect. Particle deposition patterns between both sides of the airways are more evenly distributed after surgery. These findings suggest that correcting anatomic deformities may improve intranasal medication delivery. For enhanced particle penetration, patients with nasal deformities may explore different nozzle positions.

Keywords

Computational fluid dynamics; Computer Modeling for Nasal Airflow; Allergic rhinitis; Topical Therapy for Chronic Rhinosinusitis; Post-Operative

Address Correspondence to: Dennis O. Frank, Ph.D., Department of Otolaryngology/Head and Neck Surgery, University of North Carolina at Chapel Hill, 170 Manning Drive, CB #7070, Chapel Hill, NC 27599, dennis_frank@med.unc.edu, Phone: (919) 843-4589, Fax: (919) 966-7941.

There is no conflict of interest by any of the authors.

INTRODUCTION

Topical administrations of intranasal medication are usually given by nasal drops, aqueous spray pumps, and nebulizers. A combination of drug, device, and patient factors can contribute to the efficacy of intranasal drugs. These include drug formulation characteristics, delivery device design, delivery technique, site of deposition, nasal anatomy, and underlying sinonasal medical conditions.[1,2] Nasal anatomy is particularly significant since it is characterized by variations across individuals. For subjects with nasal anatomic deformities associated with nasal airway obstruction (NAO), deposition efficacy of aqueous spray pumps have not been well described.

NAO is a common health condition known to affect all age groups and can negatively impact mood, energy, recreation, sleep and overall quality of life.[3] The prevalence of an anatomic deformity such as deviated nasal septum in healthy adults is approximately 19.5–26%.[4] Allergic rhinitis and chronic rhinosinusitis, two conditions frequently treated with topical intranasal medications, are common conditions estimated to affect 10–25% of the general population.[5,6] Therefore, it is very likely that many patients have co-existing anatomic deformities and allergic/inflammatory conditions contributing to nasal obstruction. However, there is sparse or no information in the literature about the effects of a septal deviation or other anatomic deformities on delivery of topical medication to the areas of the nasal cavity where it will have its greatest effect nor any reports of whether surgical correction of such underlying anatomic deformity improve the efficacy of topical medication.

With the availability of powerful bioengineering computer-aided design software, anatomically-accurate, three dimensional (3D) computational models can be generated from patient-specific digital data such as computed tomography (CT) scan images. Computational fluid dynamics (CFD) techniques can be used to simulate the flow of air, heat transfer, air humidification, and particulate transport through the 3D reconstructed nasal geometry.[4,6–14]

In a previous pilot study,[7] we compared drug delivery penetration past the nasal valve of a septal deviated patient using simulated aqueous spray pumps or nebulizers. However, the study was limited to a pre-operative nasal geometry. A study by Moghadas, et al. [12] investigated micro- and nano-particle transport and deposition in pre- and post-operative nasal passage models of a 25 years of male subject who underwent septoplasty. However, this study was limited to one individual. The objective of the present study was to use CFD techniques to evaluate aqueous nasal spray penetration efficiencies before and after surgical correction of intranasal anatomic deformities in five patients.

METHODS

Subjects

Two males and three females between 27 and 53 years were enrolled from the patients who presented to the Medical College of Wisconsin (MCW) Otolaryngology clinic for treatment. The inclusion criteria were: 1) 15 years old or older, 2) clinical diagnosis of non-reversible, surgically treatable cause for nasal obstruction (deviated septum, turbinate hypertrophy resistant to medical treatment, or lateral nasal wall collapse), 3) elect nasal surgery, and 4) give written informed consent. Exclusion criteria include chronic sinusitis, nasal polyposis, and other forms of sinonasal disease. The research described here was approved by the Institutional Review Board at MCW. Diagnosis of NAO and surgical treatment decisions were made by the surgeon (JSR) based on clinical presentation and the standard of medical care; all the patients were otherwise healthy.

In order to eliminate any potential effects of nasal cycling on our CFD simulations as well as avoiding sampling selection bias, the first five subjects with no obvious signs of congestion and decongestion of the nasal mucosa in both pre- and post-operative CT scans were selected in this study. The scans for all five subjects were done in 0.5mm slice increments, with number of slices ranging from 191–216 (Pre) and 142–208 (Post), and pixel sizes of 0.303–0.313 mm. To allow for adequate healing time, postoperative CT scans were performed between 5 and 8 months after surgery.

Pre-operative diagnoses revealed varying degree of moderate to severe septal deviation on all five subjects, as well as additional nasal deformities shown in Table 1. All patients underwent septoplasty and supplementary surgery consistent with their diagnoses. These procedures are designed to improve airflow at the region of the nasal valve and beyond. Post-surgical care was performed in the usual manner following nasal surgery with an uneventful post-operative course.

Nasal Model Reconstruction

Pre- and post-operative CT scans were imported into a medical imaging software package, Mimics™ 13.1 (Materialise, Inc., Plymouth, MI), and 3D reconstructions of each subject's nasal airways, excluding the paranasal sinuses, were created. The reconstructed nasal models were exported from Mimics™ in STL (stereolithography) file format into the CAD and mesh generating software package ICEM-CFD™ 12.1 (ANSYS, Canonsburg, PA). Planar nostril and outlet surfaces were constructed, and regions for tracking particle deposition were designated as follows: the anterior region, ranging from the nostrils up to the nasal valve area, the middle region, consisting of the turbinates and adjacent nasal septum, and the nasopharynx, defined as posterior to the turbinates and septum (Fig. 1A).

Airflow simulation

In order to solve the equations that govern fluid flow, computational meshes of each subject's pre- and post-surgery airways were created in ICEM-CFD™ using approximately 4 million graded tetrahedral elements, based on an in-house mesh density study indicating that about 4 million elements provides mesh independent numerical results. Three layers of prism elements were created at the nasal airway walls to accurately account for near-wall particle trajectories. CFD simulations were carried out in two uncoupled phases, airflow and particle transport.

Steady-state, laminar inspiratory airflow was simulated using the CFD software package Fluent™ 12.1.4 (ANSYS, Inc., Canonsburg, PA) under pressure-driven conditions. The boundary conditions specified in Fluent to determine the airflow field were identical to those previously used:[4,7] Briefly, these boundary conditions were: 1) a "wall" condition assuming that the walls were stationary with zero air velocity at the air-wall interface; 2) a "pressure-inlet" condition at the nostrils with gauge pressure set to zero; 3) a "pressure-outlet" condition at the outlet with gauge pressure set to a pressure drop derived for each patient that generated a pre-determined steady-state resting flow rate. This flow rate was calculated to be twice the minute volume (amount of air inhaled in 1 min, defined as tidal volume times respiratory rate) estimated from body weight using gender-specific power law curves derived by Garcia, et al. [15]

Spray specification and particle trajectories

The position of the simulated spray nozzle set to be 0.5cm into the nasal vestibule from the nostril surface on each side for every patient, and was the largest distance of those reported by Kimbell, et al. [8] that adequately fit into the nasal vestibule of all the patients. Simulated sprays were initially directed laterally or to the side, away from the septum and toward the

outer portion of the eye as recommended by Benninger, et al. [17] However, the angle from the nostril center to the outer eye aimed the spray directly onto the lateral vestibule wall in all patients and so was modified slightly to point toward the center of the eye rather than the outer corner. In addition, to investigate whether the presence of a septal deviation may require patients to alter the angle of nozzle insertion and angulation of spray pumps from the slightly modified recommended technique (Position A),[17] an alternative spray nozzle position (Position B) was tested for Subject 5, such that spray was directed by rotating the recommended nozzle position 42° inferiorly (Fig. 1B).

Simulated sprays consisted of aerosol particle sizes ranging from 10 to 110μm in aerodynamic diameter, with a spray plume angle of 68° designed to resemble the Pfeiffer spray pump PF-80 used by Cheng, et al. [18] The average velocity range of most commercially available sprays is 1 to 14.7m/s,[8,19] and the discharge velocity of flunisolide (though unknown) was estimated to be 370cm/s (3.7m/s)[20] so a simulated spray velocity of 3m/s was used here. Particle trajectories were calculated using the Discrete Phase Model in Fluent™. Particles that exited the nasal airways at the outlet via the nasopharynx were categorized as “Escaped.” For particles that deposited in the nasal cavity, the region where each particle deposited was recorded. The “solid cone” injection type was specified in Fluent™ to simulate particle streams that emanated from the spray release position at randomly dispersed angles throughout the spray cone region. To characterize particle size distribution in a polydisperse form, a Rosin Rammler Particle Size Distribution[21] set to range in aerodynamic diameter from 10 to 110μm with mean diameter of 66 μm and spread distribution parameter of 2.89 was utilized.[18] A total of 1100 particle streams were released from each nostril.

Statistical Analysis

Statistical analysis was conducted on CFD simulated data to test the null hypothesis that deviated nasal septum does not impact sprayed aerosol distribution on the obstructed side. Student’s t-test for matched pairs was used to test this null hypothesis. Pre- and post-surgery comparisons were done on anterior and posterior region deposition values and on the number of particles that by-passed the entire nasal cavity (Escaped). Posterior deposition was calculated as the sum of aerosolized particles that deposited in the middle and nasopharynx regions.

RESULTS

Statistical tests of the null hypothesis comparing pre- and post-surgery deposition patterns in the anterior, posterior, and escaped regions are presented in Table 2. Simulations predicted that the presence of septal deviation significantly affected both anterior (p=0.01999) and posterior deposition (p=0.03591), and that there was no significant difference in the number of sprayed particles that escaped (p=0.05989) the nasal cavity on the obstructed side. CFD results on the obstructed side showed that anterior deposition decreased by 13% after surgery, while posterior deposition increased by 118% (Fig 2A). Sprayed aerosol deposition on the contralateral (unobstructed) side indicated more particle penetration into the middle and nasopharynx regions, and less anterior deposition before surgery than after (Fig. 2B). A comparison of posterior particle distribution differences between obstructed and contralateral sides of the airways were 113% and 30% for pre- and post-surgery, respectively (Fig. 2C).

Comparisons between the two different interpretations of the recommended intranasal spray technique[17] (Positions A & B) for Subject 5 are displayed in Figure 3. In the pre-operative nasal model (Fig. 3A); particle deposition patterns for the two spray positions were not vastly different, although simulation results showed that ‘Position B’ had a slight lower

anterior deposition, and more particles escaped the nasal cavity. Whereas in the post-operative nasal geometry (Fig. 3B), simulation predicted that 'Position B' had superior deposition efficiency; particle deposition in the anterior region of the nose dropped by 68%, while aerosol penetration into the middle and nasopharynx regions improved by 1944% and 215%, respectively.

DISCUSSION

The results of this study, comparing aqueous nasal spray penetration efficiencies before and after surgical correction of intranasal anatomic deformities in five NAO patients, indicate that aerosolized particle penetration improved significantly post-surgery on the anatomically obstructed side. At the same time, did not significantly impact the number of particles that bypassed the nasal cavity at the nasopharynx. Simulation data suggests that altering the angle of spray nozzle insertion may enhance aerosol particle deposition efficiency in the nasal cavity after septoplasty. CFD analysis by Wang, et al. [13] showed that particle release positions influence local deposition patterns in a healthy subject, further supporting the results of this study indicating that subjects may be well-advised to explore various spray nozzle positions. In agreement with other studies,[6,7,9,11] our simulations predicted that smaller particles had superior nasal valve penetration pre- and post-operatively in all the subjects, while larger particle sizes deposited directly into the anterior region (Fig. 4).

These results pose significant clinical implications, since the scenario of a patient with an underlying mucosal inflammatory process – e.g. rhinitis, sinusitis – coupled with an anatomical nasal deformity is a common one. The surgical correction of an underlying anatomic deformity may greatly increase the efficacy of medical management. The common management strategy of required pre-surgical nasal steroid trials for treatment of nasal obstruction symptoms may be flawed in its logic.[22] The presence of a moderate to severe septal deviation or other anatomic deformity, as was the case in all our study subjects, hinders nasal spray drug delivery, implying that the effectiveness of nasal spray usage pre-surgically is essentially suboptimal. Therefore, while no definitive conclusions can be made based on this study alone, in a patient with co-existing anatomic and inflammatory conditions one may consider proceeding with surgical planning to address the anatomic components at the time of initiating a nasal spray medication as the drug delivery will be greatly enhanced if the affected nasal passage side is normalized in its anatomical configuration, as well as creating a more even particle distribution between both sides of the nasal airways.

In this study, airflow was simulated under laminar conditions. Although nasal airflow may become turbulent at flow rates occurring during sniffing or exercise, there is evidence that laminar conditions dominate nasal air flows at resting breathing rates.[10,14] For the purposes of focusing this study on a comparison of pre- and post-surgery spray deposition, time-dependent effects of the breathing cycle were not considered. Steady-state simulation results were assumed to be representative of particle deposition over time and capable of discriminating pre- and post-surgery differences when conducted in a consistent manner as was done here. Finally, while we did demonstrate a statistically significant improvement in penetration to the more posterior portions of the nose, the study design did not allow correlation with actual patient symptoms or response to drug therapy so no definitive clinical or pharmacological conclusions can be made.

In conclusion, the present CFD comparative study of aqueous nasal spray penetration efficiencies before and after nasal surgery determined that surgical correction of nasal anatomic deformities can improve spray penetration to areas where medications can have greater effect. Further study will be necessary to find spray nozzle position(s) that can

maximize aerosolized particle penetration, a standardized recommended nozzle position may be useful as a starting point for patient education on usage of nasal sprays, but given the uniqueness of individual patient anatomy, our results suggest that alterations in spray nozzle position may be needed to optimize intranasal drug delivery.

Acknowledgments

This research was funded by grants R01EB009557 and R01EB009557-01S1 from the National Institutes of Health/ National Institute of Biomedical Imaging and Bioengineering, under subcontract to the University of North Carolina from the Medical College of Wisconsin. This description of results from this research is solely the responsibility of the authors and does not represent the official views of the NIH. The authors thank Nicole Stelse for her contributions to this work.

References

1. Merkus P, Ebbens FA, Muller B, Fokkens WJ. Influence of anatomy and head position on intranasal drug deposition. Eur Arch Otorhinolaryngol. 2006; 263:827–832. [PubMed: 16807754]
2. Blaiss MS, Benninger MS, Fromer L, et al. Expanding choices in intranasal steroid therapy: summary of a roundtable meeting. Allergy Asthma Proc. 2006; 27:254–264. [PubMed: 16913270]
3. Rhee JS, Book DT, Burzynski M, Smith TL. Quality of life assessment in nasal airway obstruction. Laryngoscope. 2003; 113:1118–1122. [PubMed: 12838007]
4. Garcia GJM, Rhee JS, Senior BA, Kimbell JS. Septal deviation and nasal resistance: An investigation using virtual surgery and computational fluid dynamics. Am J Rhinol Allergy. 2009; 24:e46–53. [PubMed: 20109325]
5. Aggarwal R, Cardozo A, Homer JJ. The assessment of topical nasal drug distribution. Clinical otolaryngology and allied sciences. 2004; 29:201–205. [PubMed: 15142061]
6. Chen XB, Lee HP, Chong VF, Wang de Y. A computational fluid dynamics model for drug delivery in a nasal cavity with inferior turbinate hypertrophy. Journal of aerosol medicine and pulmonary drug delivery. 2010; 23:329–338. [PubMed: 20804427]
7. Frank DO, Kimbell JS, Pawar S, Rhee JS. Effects of Anatomy and Particle Size on Nasal Sprays and Nebulizers. Otolaryngology--head and neck surgery: official journal of American Academy of Otolaryngology-Head and Neck Surgery. 2011
8. Kimbell JS, Segal RA, Asgharian B, et al. Characterization of deposition from nasal spray devices using a computational fluid dynamics model of the human nasal passages. J Aerosol Med. 2007; 20:59–74. [PubMed: 17388754]
9. Schroeter, JD.; Tewksbury, EW.; Kimbell, JS. Experimental and Computational Predictions of Particle Deposition in a Sectional Human Nasal Model. In: Dalby, RN.; Byron, PR.; Peart, J.; Suman, JD.; Farr, SJ.; Young, PM., editors. Respiratory Drug Delivery 2008. Richmond, VA: Virginia Commonwealth University; 2008. p. 763-766.
10. Garlapati RR, Lee HP, Chong FH, Wang DY. Indicators for the correct usage of intranasal medications: A computational fluid dynamics study. Laryngoscope. 2009; 119:1975–1982. [PubMed: 19655385]
11. Inthavong K, Tian ZF, Tu JY, et al. Optimising nasal spray parameters for efficient drug delivery using computational fluid dynamics. Comp Biol Med. 2008; 38:713–726.
12. Moghadas H, Abouali O, Faramarzi A, Ahmadi G. Numerical investigation of septal deviation effect on deposition of nano/microparticles in human nasal passage. Respiratory physiology & neurobiology. 2011; 177:9–18. [PubMed: 21402179]
13. Wang SM, Inthavong K, Wen J, et al. Comparison of micron- and nanoparticle deposition patterns in a realistic human nasal cavity. Respiratory physiology & neurobiology. 2009; 166:142–151. [PubMed: 19442930]
14. Shanley KT, Zamankhan P, Ahmadi G, et al. Numerical simulations investigating the regional and overall deposition efficiency of the human nasal cavity. Inhalation toxicology. 2008; 20:1093–1100. [PubMed: 18800272]

15. Garcia GJM, Schroeter JD, Segal RA, et al. Dosimetry of nasal uptake of water-soluble and reactive gases: A first study of interhuman variability. Inhal Toxicol. 2009; 21:607–618. [PubMed: 19459775]

16. Beals JA, Funk LM, Fountain R, Sedman R. Quantifying the distribution of inhalation exposure in human populations: distribution of minute volumes in adults and children. Environmental health perspectives. 1996; 104:974–979. [PubMed: 8899377]

17. Benninger MS, Hadley JA, Osguthorpe JD, et al. Techniques of intranasal steroid use. Otolaryngol Head Neck Surg. 2004; 130:5–24. [PubMed: 14726906]

18. Cheng YS, Holmes TD, Gao J, et al. Characterization of nasal spray pumps and deposition pattern in a replica of the human nasal airway. J Aerosol Med. 2001; 14:267–280. [PubMed: 11681658]

19. Suman JD, Laube BL, Lin TC, et al. Validity of in vitro tests on aqueous spray pumps as surrogates for nasal deposition. Pharmaceutical research. 2002; 19:1–6. [PubMed: 11837692]

20. Hallworth GW, Padfield JM. A comparison of the regional deposition in a model nose of a drug discharged from metered aerosol and metered-pump nasal delivery systems. The Journal of allergy and clinical immunology. 1986; 77:348–353. [PubMed: 3944385]

21. Rosin P, Rammler E. The laws governing the fineness of powdered coal. Journal of the Institute of Fuel. 1933; 7:29–36.

22. Rhee JS. Measuring outcomes in nasal surgery: realities and possibilities. Archives of facial plastic surgery: official publication for the American Academy of Facial Plastic and Reconstructive Surgery, Inc and the International Federation of Facial Plastic Surgery Societies. 2009; 11:416–419.

23. Schroeter JD, Kimbell JS, Asgharian B, et al. Computational fluid dynamics simulations of submicrometer and micrometer particle deposition in the nasal passages of a Sprague-Dawley rat. Journal of aerosol science. 2011; 43:31–44.

24. Dowley AC, Homer JJ. The effect of inferior turbinate hypertrophy on nasal spray distribution to the middle meatus. Clinical otolaryngology and allied sciences. 2001; 26:488–490. [PubMed: 11843929]

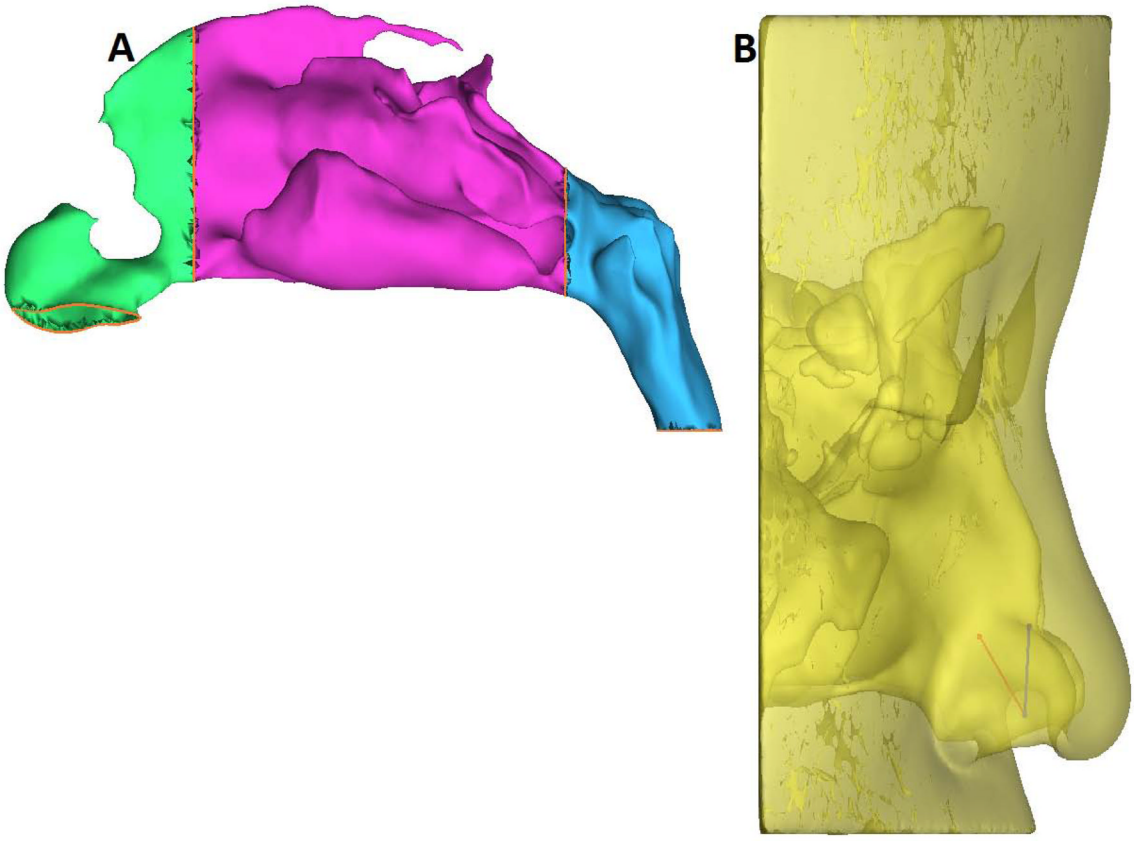

Figure 1.
(A)Sagittal view of the obstructed side of the nasal passage showing regions used for tracking particle deposition (green, anterior; purple, middle; blue, nasopharynx).
(B) Nozzle positions based on the recommended technique[17] showing superior (Position A) spray axis and release point (blue), and inferior (Position B) spray axis and release point (red) in Subject 5.

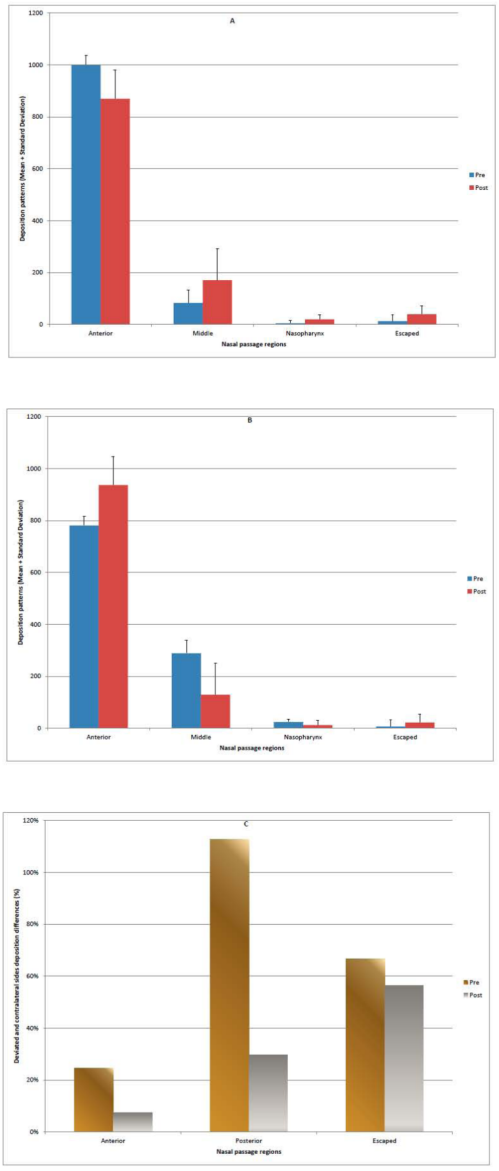

Figure 2.

Pre- and post-operative regional deposition patterns on the obstructed side of the nasal passage.

(A) Obstructed side (means + standard deviation).

(B) Unobstructed side (means + standard deviation).

(C) Deposition differences between obstructed and contralateral sides (*Posterior deposition= middle + nasopharynx*).

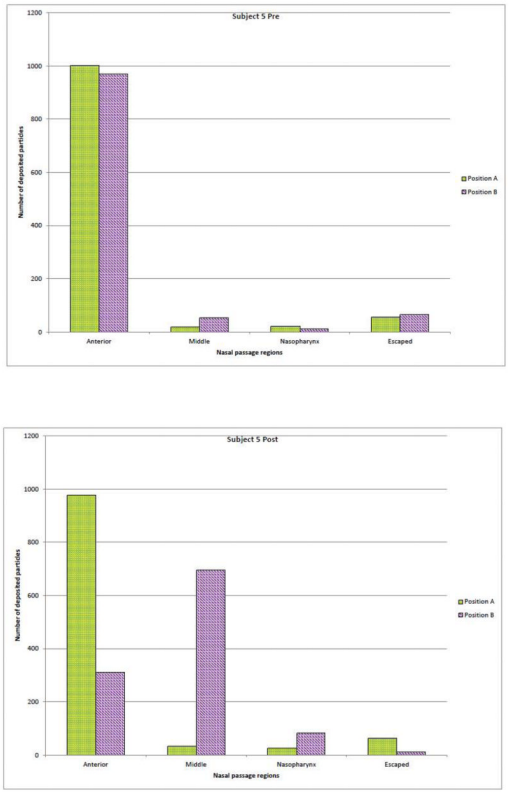

Figure 3.
Regional deposition patterns (Subject 5) with respect to nasal spray pump nozzle positions A and B, respectively.
(A)Pre-surgery
(B) Post-surgery

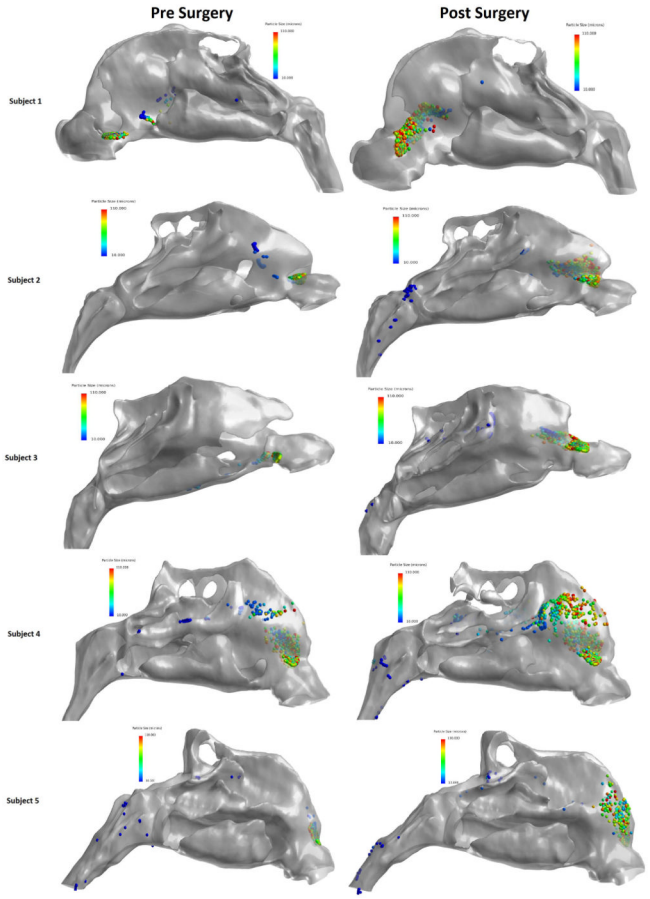

Figure 4.
Pre- and post-operative spatial deposition patterns.

Table 1

Patients' diagnoses and surgical intervention

Subject	Diagnoses	Predominate side of obstruction	Performed procedure
1	Deviated nasal septum External nasal deformity	Left	Septorhinoplasty
2	Deviated nasal septum External nasal deformity Inferior turbinate compensatory hypertrophy	Right	Septorhinoplasty Left inferior turbinectomy
3	Deviated nasal septu External nasal deformit Inferior turbinate compensatory hypertrophy	Right	Septorhinoplasty Left inferior turbinectomy
4	Bilateral vestibular stenosis Deviated nasal septum Bilateral inferior turbinate hypertrophy	Right	Bilateral vestibular stenosis repaired with butterfly onlay graft Septoplasty Bilateral inferior turbinate turbinectomy
5	Deviated nasal septum Inferior turbinate compensatory hypertrophy Left middle turbinate concha bullosa	Right	Septoplasty Left inferior turbinectomy Left middle turbinate concha bullosa resection

Table 2

Test of hypothesis that deviated nasal septum does not impact sprayed aerosol distribution on the deviated side for n=5. Pre and post-surgery regional particle deposition patterns are presented as *means ± standard deviation*. Statistical comparisons were carried out using Student's t-test for matched pairs. P-value<0.05 indicate statistical significance (all cases).

Region	Pre	Post	P-value
Anterior	999.8±36.1	869.8±111.1	0.01999
Posterior	87.4±43.0	190.4±113.9	0.03591
Escaped	12.8±24.9	39.6±33.0	0.05989